

Determination of Reactance Loading for Circularly Polarized Circular Loop Antennas With a Uniform Traveling-Wave Current Distribution

RongLin Li, *Senior Member, IEEE*, Nathan A. Bushyager, *Member, IEEE*, Joy Laskar, *Fellow, IEEE*, and Manos M. Tentzeris, *Senior Member, IEEE*

Abstract—A simple theory is presented to predict the lumped reactance loading for circularly polarized circular loop antennas with a uniform traveling-wave current distribution. The reactive load is located on a circular wire loop of one-wavelength circumference at a position of 45° away from the feed point. To achieve a uniform traveling-wave current distribution, the loading reactance and the input impedances of the loaded and unloaded loop antennas need to satisfy certain conditions. First, the input resistance and the input reactance of the unloaded loop antenna should have the same absolute value. Second, the input impedance of the loaded loop must be purely resistive and its value needs to be two times of the input resistance of the unloaded loop. Third, the loading reactance should be chosen to be two times in value and opposite in sense of the input reactance of the unloaded loop. These conditions can be approximately met when the circular loop is placed above a ground plane. The loading reactance is determined from the input impedance of the unloaded loop and is optimized for an optimal performance of circular polarization. It is found that the reactive load must be capacitive and its value depends on the height of the loop above the ground plane and the thickness of the wire. The characteristics of the circular polarization and the input impedance of the capacitance-loaded circular loop antennas are investigated. An experimental example is presented to verify the theoretical prediction.

Index Terms—Circular loop antenna, circular polarization, reactively loaded antenna, uniform traveling-wave current distribution.

I. INTRODUCTION

IT IS well-known that a single-fed circular wire loop antenna of one-wavelength circumference (called one-wavelength loop in short) creates a standing-wave current distribution and thus radiates a linearly polarized wave in the far-field zone [1]–[3]. It is also easy to understand that a one-wavelength circular loop can radiate perfectly circularly polarized waves in the direction perpendicular to the plane of the loop if a uniform traveling-wave current distribution is generated [4]. A common way to produce a uniform traveling-wave current distribution is to feed the loop antenna with two 90° phase shifted generators which are located 90° (or a quarter-wavelength) apart along the loop so that a superposition of two standing-wave

current distributions with equal amplitude, 90° phase shift in time, and a quarter-wavelength difference in space results in a perfectly uniform traveling-wave current distribution [5]. The disadvantage of this approach is the need for two sources or a 90° hybrid coupler. Another commonly used technique for achieving a traveling-wave current distribution is to load the antenna with resistors [6]. Obviously the main problem of this method is that it leads to low antenna efficiency since the resistors absorb the majority of fed power. In the 1980s, it was demonstrated that a traveling-wave current distribution could be obtained if a circular loop is reactively loaded at a position of 45° away from the feed point [7]. However, it was shown in [7] that the obtained traveling-wave current distributions were far from uniform due to the high-value (>300 ohms) of the used reactance. (High-value impedance loading usually tends to block the flowing of current, thus causing a dip in the magnitude of the current distribution.) In addition, the loaded loop antenna usually needs to be placed at a considerable height above a ground plane (e.g., at a height of more than a quarter-wavelength considered in [7]) and results in a high input impedance (e.g., input resistance >200 ohms and input reactance <-200 ohms), thus causing difficulties in matching the antenna to the feeding system. Most importantly, no theoretical prediction has been given in [7] for the value of the loading reactance; therefore it was not clear why a traveling-wave current distribution could be achieved by the reactive load.

It is our purpose here to demonstrate that it is possible to theoretically predict the loading reactance for the launching of a uniform traveling-wave current distribution along a one-wavelength circular loop antenna. It will be proven that there are simple relationships among the loading reactance and the input impedances of the loaded and unloaded loop antennas. Also, it will be found that the uniform traveling-wave current distribution can be created when a one-wavelength circular loop is situated at a height of much less than a quarter-wavelength (about 0.05–0.15 wavelengths considered in this paper) above the ground plane. Thus, the low-profile circular loop antenna can be loaded with a low-value capacitive reactance, leading to smaller input impedance which facilitates the matching of the antenna.

This paper is organized as follows. First, the conditions for a uniform traveling-wave current distribution will be derived. Then, the uniform traveling-wave current distribution will be realized by placing a circular wire loop over a ground plane. The

Manuscript received November 1, 2004; revised April 30, 2005. This paper was supported in part by NSF CAREER Award ECS-9984761 and in part by NSF Grant ECS-0313951.

The authors are with the Georgia Electronic Design Center, School of Electrical and Computer Engineering, Georgia Institute of Technology, Atlanta, GA 30332-0250 USA (e-mail: rlli@ece.gatech.edu).

Digital Object Identifier 10.1109/TAP.2005.859767

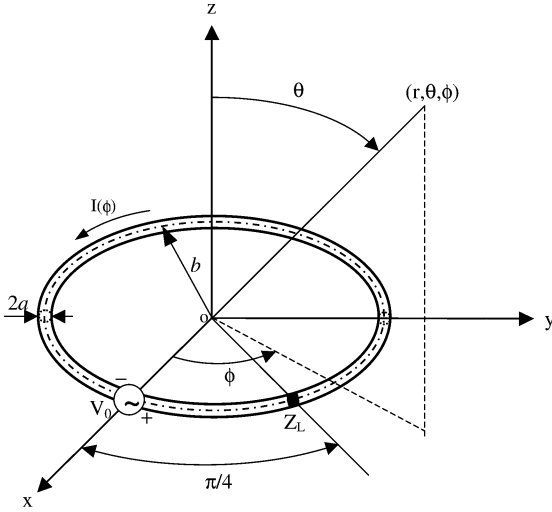


Fig. 1. Geometry of a circular loop antenna loaded at $\phi = \pi/4$ with impedance Z_L .

characteristics of input impedance and circular polarization will be investigated. Finally, a comparison of simulated and measured results will be performed.

II. CONDITIONS FOR A UNIFORM TRAVELING-WAVE CURRENT DISTRIBUTION

Consider a lossless circular wire loop antenna (shown in Fig. 1) with a loop radius of b and a wire radius of a . It is assumed that the circumference of the loop is one wavelength (λ_0), i.e., $kb = 1.0$ ($k = 2\pi/\lambda_0$), and that the wire radius satisfies the “thin wire” approximation, i.e., $ka < 0.1$ [8]. The loop is fed by a voltage source V_0 at $\phi = 0$ and is loaded by a lumped impedance Z_L at $\phi = \pi/4$. Under the “thin wire” approximation, the current distribution on the loop can be represented by a filamentary current $i(\phi, t) = I(\phi)e^{j\omega t}$ along the loop circumferential axis. We assume a uniform traveling-wave current distribution created on the loop such that [9], [10]

$$I(\phi) = I_0 e^{\pm j\phi} \quad (1)$$

where the plus sign (the upper part of the symbol “ \pm ”) is used for a left-hand (with thumb in the $+z$ direction) traveling-wave current distribution and the minus sign (the lower part of the symbol “ \pm ”) is used for a right-hand traveling-wave current distribution. Applying the compensation theorem, we can replace the load Z_L with an equivalent loading voltage V_L [11], [12]

$$V_L = -Z_L I(\pi/4) = -Z_L I_0 e^{\pm j\pi/4}. \quad (2)$$

According to the principle of superposition [13], the current distribution $I(\phi)$ can be obtained by the superposition of the two currents in the loop when fed by each voltage source alone, that is

$$I(\phi) = I^0(\phi) + I^L(\phi) \quad (3)$$

where $I^0(\phi)$ and $I^L(\phi)$ are generated by the feeding voltage V_0 at $\phi = 0$ and the loading voltage V_L at $\phi = \pi/4$, respectively,

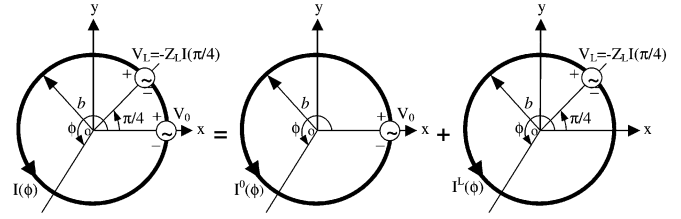


Fig. 2. Current distribution on a loaded circular loop antenna is equal to a superposition of the currents generated by the feeding voltage V_0 and the loading voltage V_L .

as illustrated in Fig. 2. It is a reasonable approximation to represent these current distributions on a single-fed one-wavelength circular loop with a cosinusoidal variation [12], [14]

$$I^0(\phi) = I_0^0 \cos(\phi) \quad (4a)$$

$$I^L(\phi) = I_0^L \cos(\phi - \pi/4). \quad (4b)$$

With the input impedance of the circular loop antenna without the load, Z_{in}^U (simply called “unloaded input impedance”), the current constants I_0^0 and I_0^L are given by

$$I_0^0 = V_0 / Z_{in}^U \quad (5a)$$

$$I_0^L = V_L / Z_{in}^U = -Z_L I_0^0 e^{\pm j\pi/4} / Z_{in}^U. \quad (5b)$$

[Note that $V_L = -Z_L I_0^0 e^{\pm j\pi/4}$ from (2)]. Substituting (4) in (3) with I_0^0 and I_0^L from (5) leads to

$$I(\phi) = \frac{V_0}{Z_{in}^U} \cos \phi - I_0^0 e^{\pm j\pi/4} \frac{Z_L}{Z_{in}^U} \cos(\phi - \pi/4). \quad (6)$$

Substituting $I(\phi) = I_0 e^{\pm j\phi}$ into the left side of (6) and replacing I_0 with $I_0 = V_0 / Z_{in}^L$, where Z_{in}^L is the input impedance of the circular loop antenna with the load (simply called “loaded input impedance”) we obtain

$$\frac{V_0}{Z_{in}^L} e^{\pm j\phi} = \frac{V_0}{Z_{in}^U} \cos \phi - \frac{V_0}{Z_{in}^U} \frac{Z_L}{Z_{in}^U} e^{\pm j\pi/4} \cos(\phi - \pi/4). \quad (7)$$

Dividing on both sides of (7) by V_0 / Z_{in}^L and moving Z_L to the left side and $e^{\pm j\phi}$ to the right side, we obtain the solution for the loading impedance:

$$Z_L = Z_{in}^U \frac{(Z_{in}^L / Z_{in}^U) \cos \phi - e^{\pm j\phi}}{e^{\pm j\pi/4} \cos(\phi - \pi/4)}. \quad (8)$$

After a simple algebra manipulation, (8) becomes

$$Z_L = 2Z_{in}^U \frac{(Z_{in}^L / Z_{in}^U - 1) \cos \phi \mp j \sin \phi}{(1 \pm j)(\cos \phi + \sin \phi)}. \quad (9)$$

Since Z_L (fixed at $\phi = \pi/4$) is independent of ϕ , we must have

$$(Z_{in}^L / Z_{in}^U - 1) = \mp j. \quad (10)$$

Therefore we obtain the precondition for a uniform traveling-wave current distribution specified on the one-wavelength circular loop, that is

$$Z_{in}^L = (1 \mp j) Z_{in}^U \text{ or } Z_{in}^U = \frac{1 \pm j}{2} Z_{in}^L. \quad (11)$$

This means that in order to realize a uniform traveling-wave current distribution, the loaded and unloaded input impedances of the circular loop antenna must be subject to a certain relationship given by (11). As a consequence of the precondition (11), we can find by substituting (10) in (9) the value of the loading impedance Z_L

$$Z_L = -(1 \pm j)Z_{in}^U \text{ or } Z_L = \mp jZ_{in}^L \quad (12)$$

which is also considered as the implementation condition for the uniform traveling-wave current distribution.

Now let us check whether a uniform traveling-wave current distribution can be really achieved if the precondition (11) and the implementation condition (12) are satisfied. Substituting (11) for Z_{in}^U and (12) for Z_L in (6) and considering $I_0 = V_0/Z_{in}^L$, we obtain

$$I(\phi) = I_0 \left[\frac{2}{1 \pm j} \cos \phi + (1 \pm j)e^{\pm j\pi/4} \cos(\phi - \pi/4) \right]. \quad (13)$$

The above equation can be further simplified as

$$\begin{aligned} I(\phi) &= I_0 [(1 \mp j) \cos \phi \pm j(\cos \phi + \sin \phi)] \\ &= I_0 (\cos \phi \pm j \sin \phi) \\ &= I_0 e^{\pm j\phi} \end{aligned} \quad (14)$$

which indeed confirms a uniform traveling-wave current distribution.

For a purely reactive load, Z_L can be expressed as

$$Z_L = jX_L \text{ for an inductive load} \quad (15a)$$

or

$$Z_L = -jX_L \text{ for a capacitive load} \quad (15b)$$

where X_L is a positive real number. Substituting (15) in the left side of (12) gives

$$X_L = (j \mp 1)Z_{in}^U \text{ or } X_L = \mp Z_{in}^L \text{ for an inductive load} \quad (16a)$$

or

$$X_L = (-j \pm 1)Z_{in}^U \text{ or } X_L = \pm Z_{in}^L \text{ for a capacitive load.} \quad (16b)$$

To guarantee the right side of (16) being equal to a positive number, we have the following observations:

- 1) For an inductive load, the input resistance and the input reactance of the unloaded circular loop antenna must have the same absolute value but with an opposite sign, that is

$$Z_{in}^U = R_{in}^U + jX_{in}^U \text{ with } R_{in}^U = -X_{in}^U. \quad (17)$$

- 2) There only exists a right-hand traveling-wave current distribution for the inductive load since we have to choose the lower part of the symbol “ \mp ” in (16a).
- 3) For a capacitive load, the input resistance and input reactance of the unloaded circular loop antenna must have the same value, that is

$$Z_{in}^U = R_{in}^U + jX_{in}^U \text{ with } R_{in}^U = X_{in}^U. \quad (18)$$

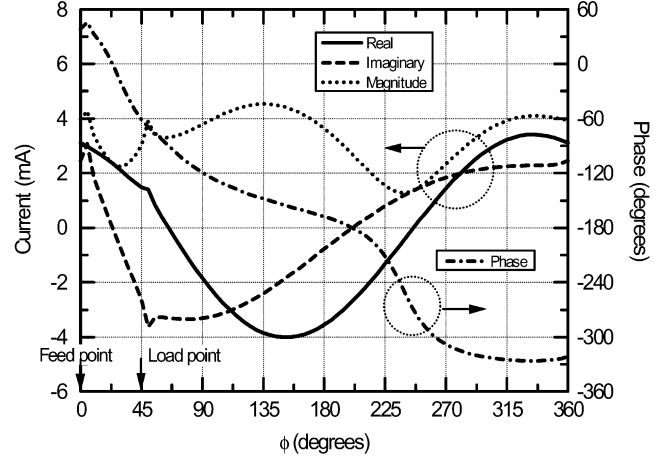


Fig. 3. Current distribution on an isolated circular loop antenna loaded by an inductance with $Z_L = j194$ ohms at $\phi = \pi/4$ [$V_0 = 1$ volt, $\Omega = 2 \ln(2\pi b/a) = 10$], showing a bad traveling-wave current distribution.

- 4) There only exists a left-hand traveling-wave current distribution for the capacitive load since we have to choose the upper part of the symbol “ \pm ” in (16b).
- 5) The value of the loading reactance should be equal to the summation of the absolute values of the unloaded input resistance and input reactance or simply equal to two times of the unloaded input resistance since the unloaded input resistance and reactance have the same absolute value, i.e., $X_L = |R_{in}^U| + |X_{in}^U| = 2R_{in}^U$.
- 6) The input impedance of the loaded circular loop antenna must be a real number and its value has to be equal to the value of the loading reactance, namely, $Z_{in}^L = X_L$.

It should be noted that loading a one-wavelength circular loop antenna with $X_L = |R_{in}^U| + |X_{in}^U|$ does not automatically result in a uniform traveling-wave current distribution even though the unloaded input impedance meets $|R_{in}^U| = |X_{in}^U|$ as required by Observations 1) and 3). Whether a uniform traveling-wave current distribution can be really realized also depends on the loaded input impedance, i.e., the precondition (11). As an example, let us consider an isolated circular loop antenna in air. For a one-wavelength circular loop with $\Omega = 2 \ln(2\pi b/a) = 10$, it is easy to find by numerical simulation (e.g., the method of moment, MoM) or from references (e.g., [15]) that the unloaded input impedance is about $Z_{in}^U = (98 - j96)$ ohms (obtained here using NEC 1.1), approximately satisfying the condition $R_{in}^U = -X_{in}^U$ for an inductive load, i.e., satisfying Observation 1). Now we load the loop with a lumped inductance with $Z_L = j194$ ohms (i.e., $X_L = |R_{in}^U| + |X_{in}^U|$) at $\phi = \pi/4$ and obtain the current distribution along the loop, as shown in Fig. 3. We can see that the current distribution indeed presents some right-hand traveling-wave features but it differs significantly from a satisfactory uniform traveling-wave current. The reason for this current distribution is the high imaginary part of the current at the feed point, which leads to a considerable reactive component in the loaded input impedance. In fact it is found that the loaded input impedance is approximately equal to $Z_{in}^L = (163 - j167)$ ohms, which by no means is a purely real impedance as noted at Observation 6). In

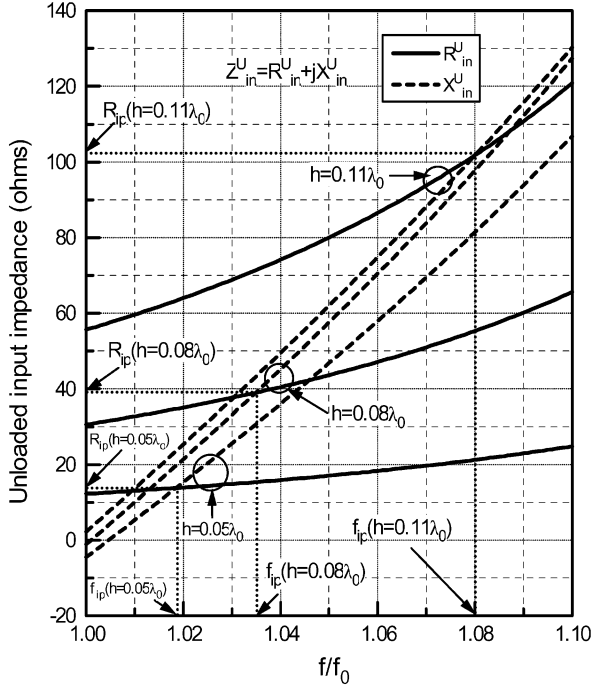


Fig. 4. Unloaded input impedance ($Z_{in}^U = R_{in}^U + jX_{in}^U$) of a circular loop antenna above a ground plane, which shows intersection points where $R_{in}^U = X_{in}^U$ ($\Omega = 10$).

general, it is difficult to control the loaded input impedance while the loading reactance is fixed at $X_L = |R_{in}^U| + |X_{in}^U|$. Fortunately an approximate solution can be found by placing the circular loop over a ground plane as introduced in [7], but the spacing between the loop and the ground plane should be much smaller than those adopted in [7] to meet the conditions for a uniform traveling-wave current distribution.

III. IMPLEMENTATION OF UNIFORM TRAVELING-WAVE CURRENT DISTRIBUTIONS

Consider a one-wavelength circular loop ($kb = 1.0$) antenna situated above a perfectly conducting infinite ground plane. The plane of the loop is parallel to the ground plane and is placed at a height h above the ground plane. Still the loop antenna is fed at $\phi = 0$ by a voltage source V_0 ($=1$ volt) and is loaded with a lumped reactive load at $\phi = \pi/4$. It will be soon demonstrated that the loading reactance must be capacitive in order to achieve a uniform traveling-wave current distribution.

As noted at Observations 1) and 3), the unloaded input impedance must satisfy the condition either $Z_{in}^U = R_{in}^U + jX_{in}^U$ with $R_{in}^U = -X_{in}^U$ for an inductive load or $Z_{in}^U = R_{in}^U + jX_{in}^U$ with $R_{in}^U = X_{in}^U$ for a capacitive load. Therefore, we first need to exam the input impedance of an unloaded circular loop above the ground plane. Fig. 4 shows the simulated frequency responses (the frequency f is normalized to $f_0 = c/\lambda_0$ with $c = 3 \times 10^8$ m/s) of the unloaded input impedance when the loop is located at three different heights: $h = 0.05\lambda_0$, $h = 0.08\lambda_0$, and $h = 0.11\lambda_0$. (All numerical simulations performed in this section were carried out using the MoM based software NEC 1.1 with 72 linear segments.) From this figure, we can find for each height an intersection point where the input impedance is

$Z_{in}^U = R_{in}^U + jX_{in}^U$ with $R_{in}^U = X_{in}^U \equiv R_{ip}$ and the frequency (f_{ip}) at the intersection point is close to f_0 ($f_{ip} < 1.1f_0$). Since the input resistance and input reactance of the unloaded impedance at f_{ip} have the same value, the reactive load has to be capacitive according to Observation 3). It can be also predicted from Observations 4) and 5) that a left-hand uniform traveling-wave current distribution may probably be obtained at $f = f_{ip}$ if the circular loop is loaded at $\phi = \pi/4$ with a capacitive impedance $Z_L = -j2R_{ip}$. To verify the prediction, we now load the circular loop with $Z_L = -j27, -j78$, and $-j204$ ohms (all of these values are exactly equal to $-j2R_{ip}$) for $h = 0.05\lambda_0$, $h = 0.08\lambda_0$, and $h = 0.11\lambda_0$, respectively, and draw the simulated current distributions at $f = f_{ip}$ in Fig. 5(a)–(c). As expected, these current distributions show the features of a left-hand uniform traveling-wave, particularly for $h = 0.05\lambda_0$, where the magnitude of the current is almost constant and the phase varies with ϕ linearly. Of course as h increases the current distribution gradually loose some uniform traveling-wave characters. This is due to two reasons: 1) f_{ip} increase with h , thus the circumference of the circular loop is no longer equal to one wavelength (the conditions derived in the above section are for a circular loop of one-wavelength circumference.) 2) the loaded input reactance also increases with increasing height h , leading to a violation to Observation 6), which requires the loaded input impedance be a real number. It is interesting to note that the input impedance of the loaded circular loop at $h = 0.05\lambda_0$ is calculated to be $Z_{in}^L = (25 - j2)$ ohms, very close to the predicted value of 27 ohms. This is also one of the reasons why a good uniform traveling-wave current is observed at this height.

The performance of circular polarization of the capacitance-loaded circular loop is shown in Fig. 6. We can see that the minimum axial ratio (in decibel) in the $+z$ direction (on-axis) does not necessarily occur at f_{ip} . This is probably because a slightly better uniform traveling-wave current distribution is created at some frequency point slightly lower than f_{ip} where the circumference is closer to one wavelength. (The circumference of the loop was fixed at $1.0\lambda_0$, one wavelength at f_0 .) It is also noticed that the bandwidth of the axial ratio increases with h , a phenomenon similar to other antennas reflected by a ground plane, such as patch antennas. The minimum axial ratio for $h = 0.11\lambda_0$ can be optimized by further adjusting the previously calculated capacitive loading reactance. The optimized capacitive load is found to be $Z_L = -j160$ ohms. It is noticed that the bandwidth for axial ratio ≤ 3 dB demonstrates no significant change for this additional optimization. The current distribution on the circular loop with the optimized capacitive load is plotted at the operating frequency $f_{op} = 1.039f_0$ (where the minimum axial ratio appears) and is placed in Fig. 5(d) for comparison, showing a much better uniform traveling-wave current distribution. The input impedance of the loaded circular loop antenna is shown in Fig. 7 for $h = 0.05\lambda_0$, $h = 0.08\lambda_0$, and $h = 0.11\lambda_0$. The input resistance decreases as the loop moves closer to the ground because more radiation power is cancelled by the image of the loop beneath the ground plane [16]. An input resistance of around 50 ohms is observed for $h = 0.08\lambda_0$ with quite low input reactance, which would facilitate the matching of the antenna to the commonly-used

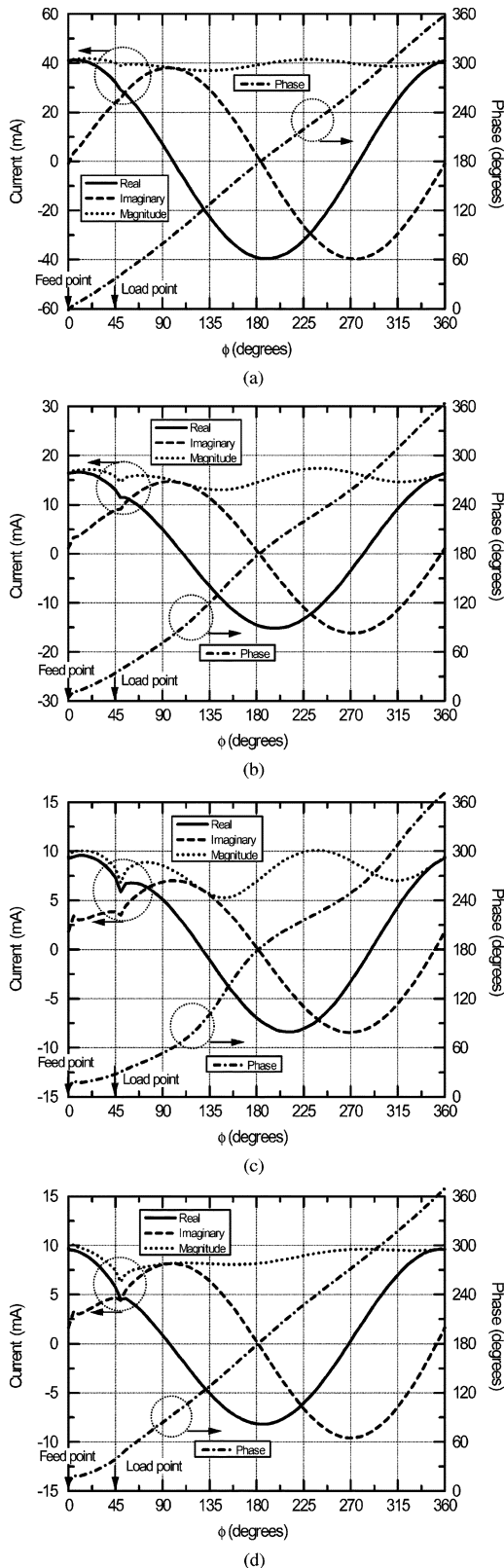


Fig. 5. Current distributions on the circular loop above a ground plane loaded with predicted capacitive reactance $Z_L = -j2R_{ip}$ for $h = 0.05\lambda_0, 0.08\lambda_0,$ and $0.11\lambda_0$ at f_{ip} , and optimized reactance $Z_L = -j160$ ohms only for $h = 0.11\lambda_0$ at f_{op} ($\Omega = 10$). (a) $h = 0.05\lambda_0$. (b) $h = 0.08\lambda_0$. (c) $h = 0.11\lambda_0$ loaded with predicted $Z_L = -j2R_{ip}$ ($-j204$ ohms) at f_{ip} . (d) $h = 0.11\lambda_0$ loaded with optimized $Z_L = -j160$ ohms at f_{op} .

50-ohms feeding system. For $h = 0.11\lambda_0$, a considerably high input reactance appears, which confirms the reason why it is

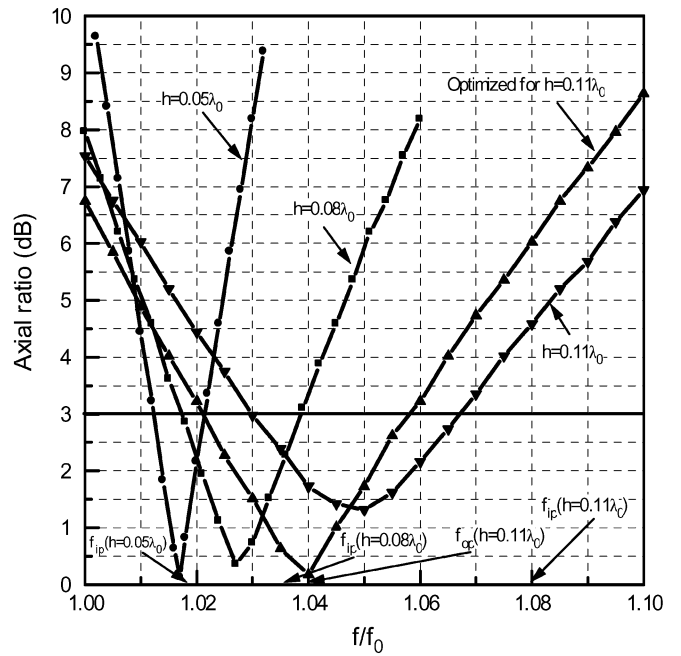


Fig. 6. Axial ratio in the $+z$ direction of the circular loop above a ground plane loaded with predicted $Z_L = -j2R_{ip}$ for $h = 0.05\lambda_0, 0.08\lambda_0,$ and $0.11\lambda_0$, and optimized capacitive reactance $Z_L = -j160$ ohms only for $h = 0.11\lambda_0$ ($\Omega = 10$).

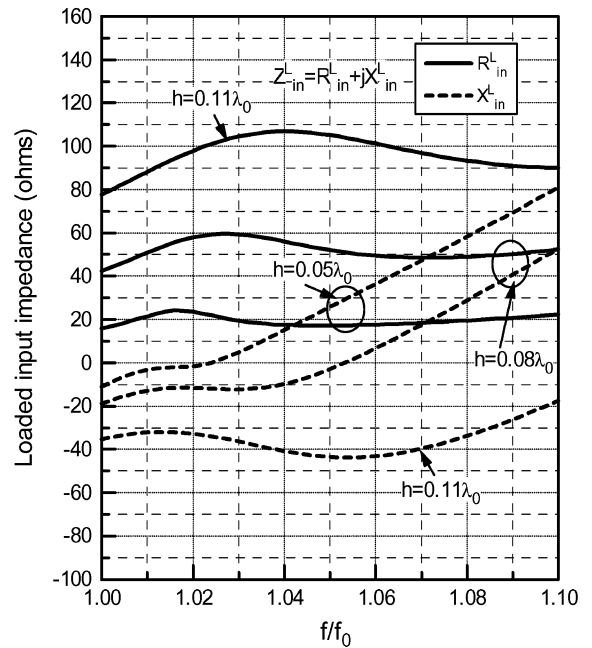


Fig. 7. Input impedance ($Z_{in}^L = R_{in}^L + jX_{in}^L$) of the circular loop antenna above a ground plane loaded with predicted capacitive reactance $Z_L = -j2R_{ip}$ ($\Omega = 10$).

more difficult at this height to achieve a uniform traveling-wave current distribution than at a lower height.

Since the value of the capacitive load and the operating frequency for a uniform traveling-wave current distribution can be predicted from the intersection point of the unloaded input resistance and input reactance, we calculated the unloaded input impedance and plotted the predicted values of the loading reactance as $X_L^L = 2R_{ip}(Z_L^L = -jX_L^L)$ and the intersection frequency f_{ip} in Fig. 8 for different heights and different loop wire

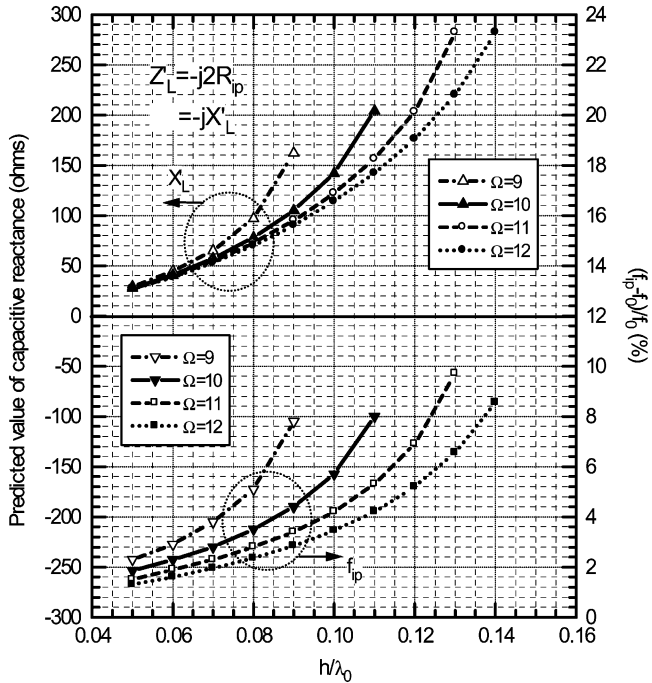


Fig. 8. Values of the capacitive reactance predicted from the intersection points of the unloaded input resistance and input reactance, and the intersection frequency f_{ip} for different heights and different loop wire thicknesses.

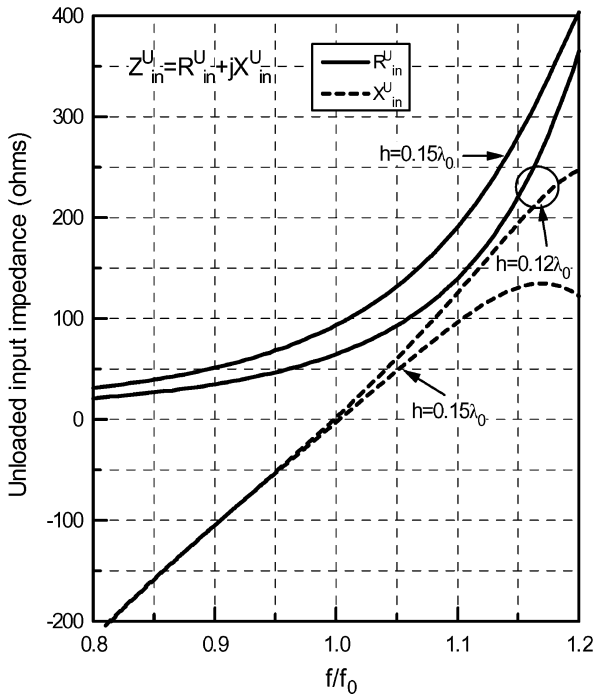


Fig. 9. Unloaded input impedance ($Z_{in}^U = R_{in}^U + jX_{in}^U$) of a circular loop antenna above the ground plane, which shows no intersection point for $h \geq 0.12\lambda_0$ ($\Omega = 10$).

thicknesses. It can be seen that the value of the loading reactance increases with the increases in the height and in the wire thickness. Also the intersection frequency shifts further away from f_0 as the height increases and/or the loop wire becomes thicker. This probably explains why a loop circumference of $1.15\text{--}1.25\lambda_0$ was selected in [7] to achieve circular polarization for the capacitively loaded circular loop at a height of a quarter-wavelength above the ground plane.

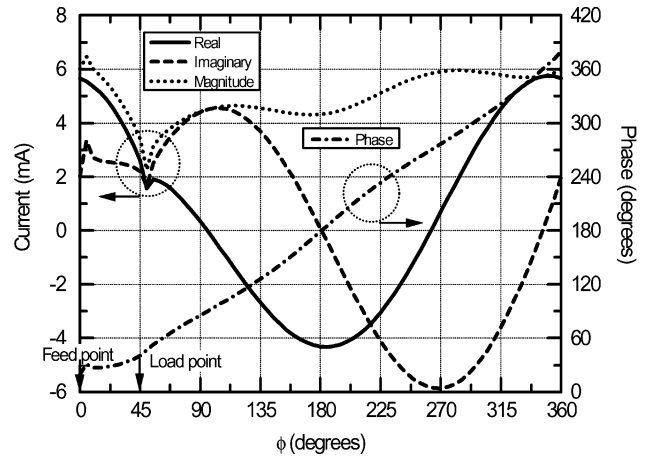


Fig. 10. Current distribution on a circular loop at a height of $h = 0.15\lambda_0$ above the ground plane loaded with optimized capacitive reactance $Z_L = -j400$ ohms ($f = 1.06$) f_0 , $\Omega = 10$, showing an obvious drop in magnitude of the current distribution at load point.

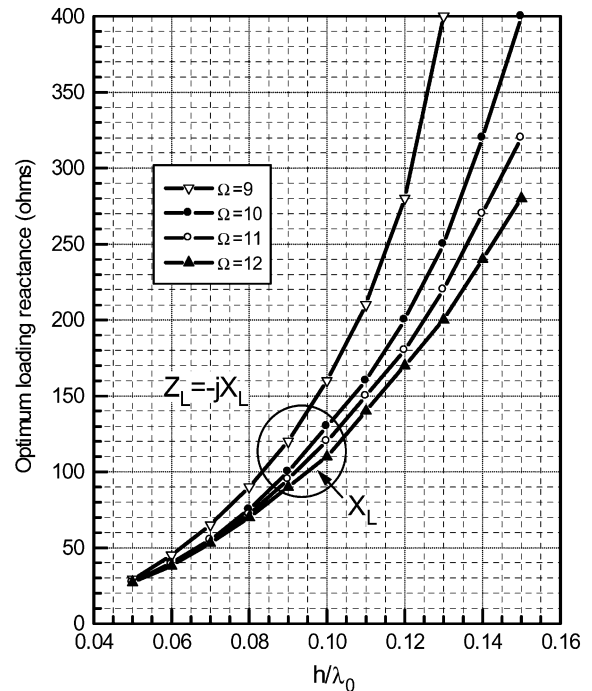


Fig. 11. Optimum loading reactance for a minimum on-axis ratio (<0.5 dB) of the circular loop antenna at different heights above a ground plane and with different wire thickness.

It should be mentioned that as the height increases beyond a certain value (e.g., $h > 0.12\lambda_0$ for $\Omega = 10$), no intersection is observed near f_0 , as illustrated in Fig. 9 where the unloaded input impedance for $h = 0.12\lambda_0$ and $0.15\lambda_0$ is plotted. But this does not mean that there is no traveling-wave current distribution for these cases. In fact, we have found a traveling-wave current distribution for $h = 0.15\lambda_0$, which is exhibited in Fig. 10. The difference for this current distribution is its less uniform magnitude (note that an obvious drop in magnitude appears at the load point.) because a higher-value capacitive reactance needs to be used as the loading. We also found that as the reactance of the capacitive load becomes higher, the performance of circular polarization of radiation patterns becomes less sensitive to the value of the loading reactance.

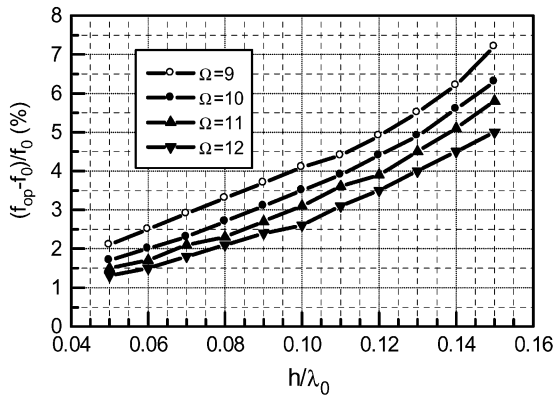


Fig. 12. Operating frequency at which the minimum on-axis axial ratio appears for the capacitance-loaded circular loop antenna at different heights above a ground plane and with different wire thickness.

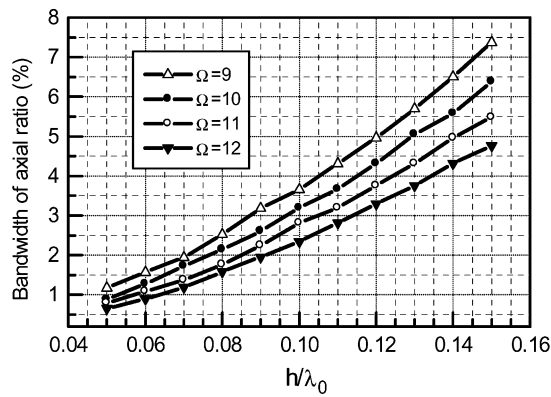


Fig. 13. Bandwidth of on-axis axial ratio (≤ 3 dB) of the capacitance-loaded circular loop antenna as a function of the loop height and wire thickness.

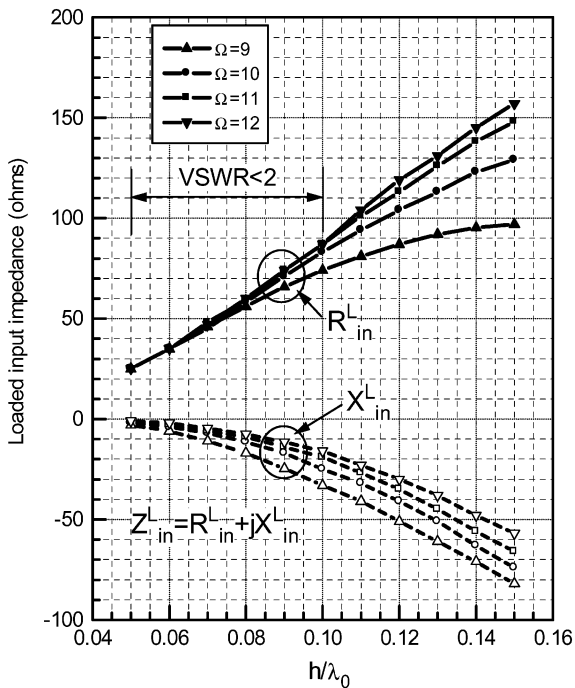


Fig. 14. Input impedance ($Z_{in}^L = R_{in}^L + jX_{in}^L$) of the capacitance-loaded circular loop antenna with different loop heights and wire thicknesses.

For example, the on-axis axial ratio ($h = 0.15\lambda_0$ and $\Omega = 10$) can remain below 1 dB even though the loading reactance varies

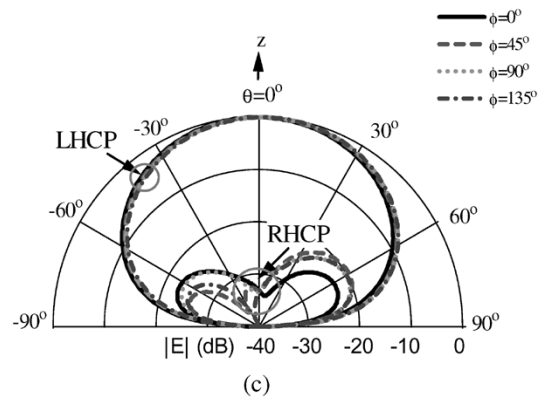
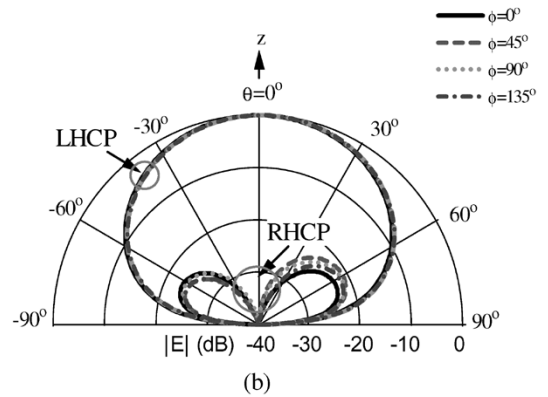
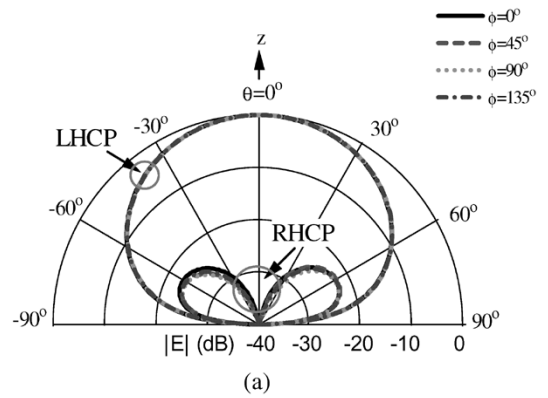


Fig. 15. Radiation patterns of the capacitance-loaded circular loop antenna on cuts $\phi = 0^\circ, 45^\circ, 90^\circ$, and 135° for $h = 0.05\lambda_0$, and $h = 0.1\lambda_0$, and $h = 0.15\lambda_0$ ($\Omega = 10$). (a) $h = 0.05\lambda_0$. (b) $h = 0.1\lambda_0$. (c) $h = 0.15\lambda_0$.

from 350 ohms to 550 ohms. In effect, for a high-value capacitive reactance, it is possible to introduce a gap on the loop for a replacement of the capacitive loading and the desirable performance of circular polarization can be achieved by adjusting the width of the gap [17].

On the basis of theoretical prediction, we optimized the capacitive loading for a minimum on-axis axial ratio (< 0.5 dB) of the circular loop antenna at different heights ($h = 0.05\text{--}0.15\lambda_0$) above the ground plane and with different wire thickness ($\Omega = 9\text{--}12$). The optimum loading reactance is plotted in Fig. 11. Comparing with Fig. 8, we find that the optimum reactance is very close to the predicted values for $h < 0.1\lambda_0$ and $\Omega \geq 10$. The operating frequency (f_{op}) at which the minimum on-axis axial ratio appears is shown in Fig. 12. We can see that the frequency shift increases with the increases in the loop height and in the wire thickness, but the maximum frequency shift is less

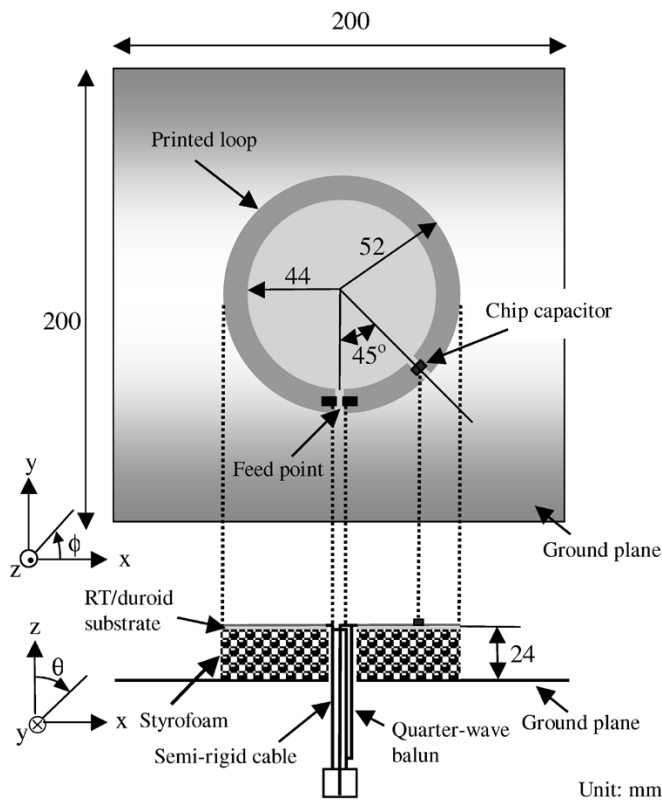


Fig. 16. Printed circular loop loaded by a capacitor at $\phi = 45^\circ$ above a finite ground plane for a uniform traveling-wave current distribution.

than 8%. The bandwidth of the on-axis axial ratio (≤ 3 dB) is depicted in Fig. 13 as a function of the loop height and the wire thickness. As expected, the bandwidth increases with increases in the loop height and in the wire thickness. The maximum axial ratio bandwidth is about 7.5% at $h = 0.15\lambda_0$ and $\Omega = 9$. The input impedance of the circular loop antenna loaded with the optimum capacitive reactance is shown in Fig. 14. It is observed that the values of both the input resistance and the input reactance increase as the loop height and the wire thickness increase. For a VSWR (voltage standing-wave ratio) of less than 2 (in a 50-ohms feeding system), the loop height should be less than $0.1\lambda_0$. The antenna gains for all the cases discussed above do not show a significant change and are found by simulation to be 9.2–9.6 dBi. The radiation patterns for $h = 0.05\lambda_0$, and $h = 0.1\lambda_0$, and $h = 0.15\lambda_0$ are plotted in Fig. 15 on cuts $\phi = 0^\circ, 45^\circ, 90^\circ$, and 135° . We can see a good symmetry with respect to the z -axis due to the uniform traveling-wave current distribution. The levels of cross-polarization (right-hand circular polarization, RHCP) are less than -20 dB compared to the co-polarization (left-hand circular polarization, LHCP).

IV. AN EXAMPLE

To verify the theoretical prediction, a capacitor-loaded circular loop antenna was fabricated and measured. The circular loop was printed on a thin dielectric substrate (substrate thickness = 0.254 mm) with a low dielectric constant (RT/duroid 5880, $\epsilon_r = 2.2$). The printed circular loop was mounted above a 200 mm \times 200 mm aluminum plate (as a finite ground plane) with the support of a piece of Styrofoam ($\epsilon_r \approx 1.03$). The design frequency was assumed to be 1 GHz.

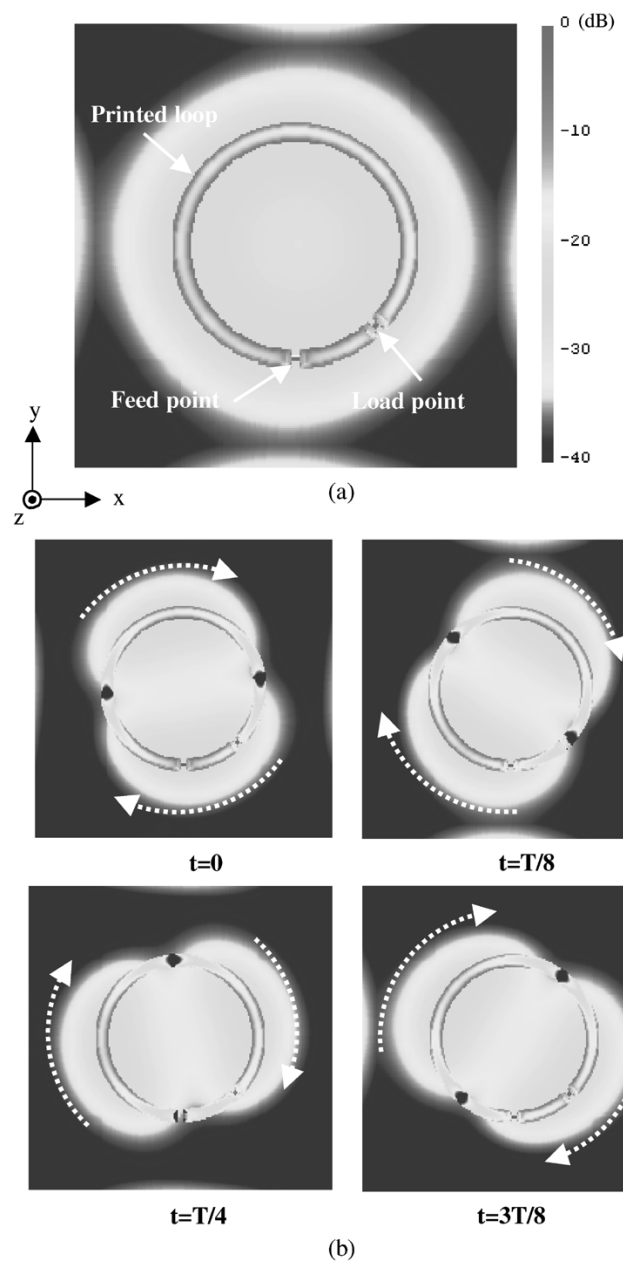


Fig. 17. Current distribution along the capacitor-loaded printed circular loop at $f = 994$ MHz ($T = 1/f$), showing a uniform left-hand rotated travelling-wave current distribution. (a) Magnitude and (b) instantaneous current.

Therefore the outer and inner radii of the printed loop were chosen to be 44 and 52 mm, respectively, to approximately model a one-wavelength wire loop with $\Omega = 10$. The height above the ground plane was selected to be $h = 0.08\lambda_0 = 24$ mm to demonstrate a very good input impedance matching. The printed loop was loaded at $\phi = 45^\circ$ by a chip capacitor with capacitance of 2.2 pF that results in a reactance of 73 ohms at 1 GHz, close to the predicted value (78 ohms) and the optimized value (75 ohms) of the capacitive loading for a uniform travelling-wave current distribution. The chip capacitor was selected from Johanson Technology Inc.'s S-Series Ultra-Low ESR Capacitors (equivalent series resistance < 0.5 ohms, self resonant frequency > 5 GHz) and fixed on the substrate using silver epoxy. The loaded printed circular loop antenna was fed

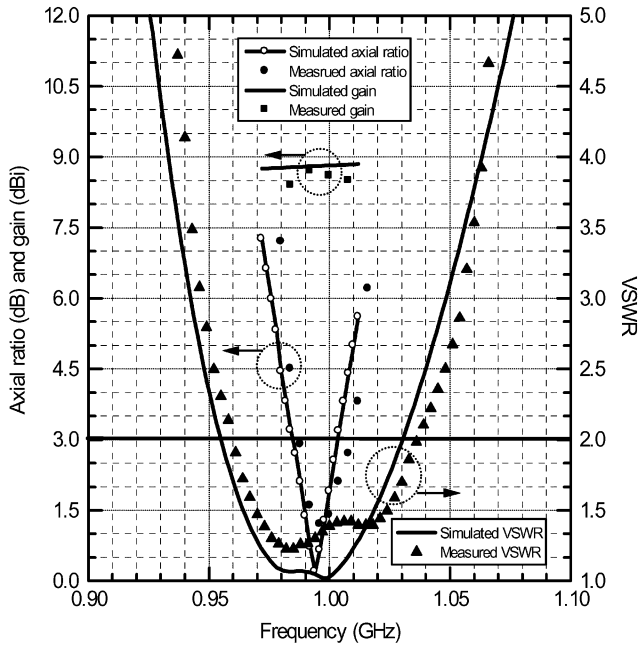


Fig. 18. Measured and simulated results of axial ratio, gain, and VSWR of the capacitor-loaded printed circular loop antenna.

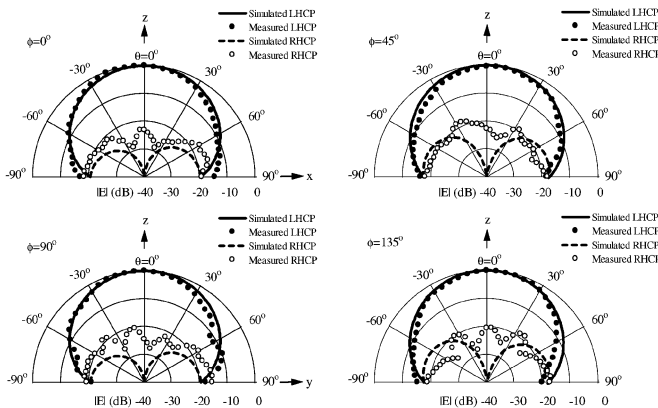


Fig. 19. Measured and simulated radiation patterns of the capacitor-loaded printed circular loop antenna ($f = 996$ MHz).

at $\phi = 0^\circ$ by a quarter-wavelength folded balun which passes through the ground plane, as illustrated in Fig. 16.

The capacitor-loaded printed circular loop antenna was simulated using Microstripes 6.5—a TLM (Transmission-Line Matrix) based full-wave EM (electromagnetic) analysis and design tool. The simulated minimum on-axis axial ratio (~ 0.2 dB) was observed at 994 MHz. The current distribution at this frequency is displayed in Fig. 17, from which we clearly see a uniform magnitude along the printed loop and a left-hand rotated traveling-wave current distribution.

The measured on-axis axial ratio, gain, and input VSWR are compared with simulation results in Fig. 18. Good agreements are obtained between the simulated and measured results. The measured minimum axial ratio was found to be 1.2 dB at 996 MHz. The bandwidth ($>5\%$) for VSWR < 1.5 is much wider than the 3-dB axial ratio bandwidth (about 2%). The antenna gain is about 8.8 dBi with a simulated radiation efficiency of higher than 98%. The radiation patterns simulated and measured at 996 MHz are plotted on cuts $\phi = 0^\circ, 45^\circ, 90^\circ$, and 135° , as shown in Fig. 19. The peak cross-polarization level is less

than -17 dB. The simulation and experiment suggest that the finite size of the ground plane has no significant effect on the performance of the capacitance-loaded circular loop antenna.

V. CONCLUSION

A theoretical prediction has been presented for determining the value of the reactance loading for a uniform traveling-wave current distribution on a circular loop of one-wavelength circumference. For a lumped reactive load located on a circular loop at a position of 45° away from the feed point, the value of the loading reactance has to be two times of the input resistance of the unloaded circular loop antenna. To achieve a uniform traveling-wave current distribution, the unloaded input resistance and input reactance must be equal in value and the loaded loop antenna should have a purely resistive input impedance with a value of two times of the unloaded input resistance. These conditions can be approximately met by placing the circular loop above a ground plane. A uniform traveling-current distribution has been achieved by loading the loop with a capacitance. The values of the capacitive loading reactance have been determined for different loop heights and loop wire thicknesses. The capacitance-loaded circular loop antennas with a uniform traveling-wave current distribution have a lower profile, more symmetrical radiation pattern, and much better input impedance matching. The numerical and experimental results have confirmed the theoretical prediction.

ACKNOWLEDGMENT

The authors wish to acknowledge the support of Georgia Electronic Design Center (GEDC) and the NSF Packaging Research Center.

REFERENCES

- [1] T. T. Wu, "Theory of thin circular loop antennas," *J. Math. Phys.*, vol. 3, pp. 1301–1304, 1962.
- [2] B. R. Rao, "Far field patterns of large circular loop antennas: Theoretical and experimental results," *IEEE Trans. Antennas Propag.*, vol. 16, no. 2, pp. 269–270, Mar. 1968.
- [3] W. L. Stutzman and G. A. Thiele, *Antenna Theory and Design*. New York: Wiley, 1998, pp. 205–210.
- [4] R. S. Elliott, *Antenna Theory and Design*. Piscataway, NJ: IEEE Press, 2003, pp. 71–73.
- [5] H. Nakano, N. Tsuchiya, T. Suzuki, and J. Yamauchi, "Loop and spiral line antennas at microstrip substrate surface," in *Proc. 6th Int. Conf. Antenna and Propagation (ICAP)*, 1989, pp. 196–200.
- [6] E. E. Altshuler, "The Traveling-wave linear antenna," *IRE Trans. Antennas Propag.*, vol. 9, pp. 324–329, Jul. 1961.
- [7] S. Okuba and S. Tokumaru, "Reactively loaded loop antennas with reflectors for circular polarization," *Trans. IECE Jpn.*, vol. J65-B, pp. 1044–1051, Aug. 1982.
- [8] R. W. P. King, "The linear antenna—eight years of progress," *Proc. IEEE*, vol. 55, pp. 2–26, Jan. 1967.
- [9] E. J. Martin, "Radiation patterns of circular loop antennas by a direct integration process," *IRE Trans. Antennas Propag.*, vol. 8, no. 1, pp. 105–107, Jan. 1960.
- [10] S. M. Prasad and B. N. Das, "A circular loop antenna with traveling-wave current distribution," *IEEE Trans. Antennas Propag.*, vol. 18, no. 2, pp. 278–280, Mar. 1970.
- [11] K. Iizuka, "The circular loop antenna multiloading with positive and negative resistors," *IEEE Trans. Antennas Propag.*, vol. 13, no. 1, pp. 7–20, Jan. 1965.
- [12] A. Shoamanesh and L. Shafai, "Characteristics of yagi arrays of two concentric loops with loaded elements," *IEEE Trans. Antennas Propag.*, vol. 28, no. 6, pp. 871–874, Nov. 1980.

- [13] J.-L. Lin and K.-M. Chen, "Minimization of backscattering of a loop by impedance loading- theory and experiment," *IEEE Trans. Antennas Propag.*, vol. 16, no. 3, pp. 299–304, May 1968.
- [14] J. E. Lindsay, "A circular loop antenna with nonuniform current distribution," *IRE Trans. Antennas Propag.*, vol. 8, pp. 439–441, Jul. 1960.
- [15] J. E. Storver, "Impedance of thin-wire loop antennas," *AIEE Trans.*, vol. 75, Nov. 1956.
- [16] A. Shoamanesh and L. Shafai, "Characteristics of circular antenna above a lossless ground plane," *IEEE Trans. Antennas Propag.*, vol. 29, no. 3, pp. 528–529, May 1981.
- [17] H. Morishita, K. Hirasawa, and T. Nagao, "Circularly polarized wire antenna with a dual rhombic loop," *Proc. Inst. Elect. Eng. Microw. Antennas Propag.*, pt. H, vol. 145, June 1998.



RongLin Li (M'02–SM'03) received the B.S. degree in electrical engineering from Xi'an Jiaotong University, China, in 1983 and the M.S. and Ph.D. degrees in electrical engineering from Chongqing University, China, in 1990 and 1994, respectively.

From 1983 to 1987, he was an Electrical Engineer with the Yunnan Electric Power Research Institute. From 1994 to 1996, he was a Postdoctoral Research Fellow with Zhejiang University, China. In 1997, he was with Hosei University, Japan, as a Hosei International Fund Research Fellow. Since 1998, he has been

a Professor with Zhejiang University. In 1999, he was a Research Associate with the University of Utah. In 2000, he was a Research Fellow with Queen's University of Belfast, U.K. In 2001, he joined the ATHENA group as a Research Scientist with the Georgia Institute of Technology, Atlanta. His latest research interests include computational electromagnetics, modeling of antennas and microwave devices, and RF packaging design.



Nathan A. Bushyager (S'99–M'05) received the B.S. degree in engineering science from The Pennsylvania State University, State College, in 1999 and the M.S. and Ph.D. degrees from The Georgia Institute of Technology, Atlanta, in 2003 and 2004, respectively.

Currently, he is a Postdoctoral Fellow with the Georgia Tech-NSF Microsystems Packaging Research Center. He has authored a book, a book chapter, six journal papers, and has presented more than 30 conference papers. His research interests include electromagnetic simulation and RF/microwave design and fabrication. His electromagnetic simulation work focuses on the wavelet based MRTD technique, statistical optimization methods, and hybrid simulators coupling mechanical and semiconductor physics with electromagnetics. In his design and fabrication work he develops multilayer RF components including filters, baluns, diplexers, phase shifters, and antennas in a variety of technologies including semiconductors, ceramic, and organic substrates.

Dr. Bushyager was the recipient of the Best Student Paper Award at the 17th Annual Review of Progress in Applied Computational Electromagnetics (ACES Society) Conference in 2001.



Joy Laskar (S'84–M'85–SM'02–F'05) received the B.S. degree in computer engineering (math/physics minors, highest honors) from Clemson University, Clemson, SC, in 1985 and the M.S. and Ph.D. degrees in electrical engineering from the University of Illinois, Urbana-Champaign, in 1989 and 1991, respectively.

Prior to joining the Georgia Institute of Technology (Georgia Tech), Atlanta, in 1995, he held faculty positions at the University of Illinois and the University of Hawaii. At Georgia Tech, he holds the

Joseph M. Pettit Professorship of Electronics, is currently the Chair for the Electronic Design and Applications Technical Interest Group, the Director of Georgia's Electronic Design Center and the System Research Leader for the NSF Packaging Research Center. In 1998, he cofounded an advanced WLAN IC Company: RF Solutions, which is now part of Anadgics (Nasdaq: Anad). In

2001, he cofounded a next generation interconnect company: Quellan, which is developing collaborative signal processing solutions for enterprise applications. He also heads a research group with a focus on integration of high-frequency electronics with optoelectronics and integration of mixed technologies for next generation wireless and optoelectronic systems. His research has focused on high frequency IC design and their integration. He has authored or coauthored more than 200 papers, several book chapters (including three textbooks in development), numerous invited talks, and has 10 patents pending.

Dr. Laskar is a 1995 recipient of the Army Research Office's Young Investigator Award, a 1996 recipient of the National Science Foundation's CAREER Award, the 1997 NSF Packaging Research Center Faculty of the Year, the 1998 NSF Packaging Research Center Educator of the Year, the 1999 corecipient of the IEEE Rappaport Award (Best IEEE Electron Devices Society Journal Paper), the faculty advisor for the 2000 IEEE MTT IMS Best Student Paper award, 2001 Georgia Tech Faculty Graduate Student Mentor of the year, recipient of a 2002 IBM Faculty Award, the 2003 Clemson University College of Engineering Outstanding Young Alumni Award and the 2003 recipient of the Outstanding Young Engineer of the Microwave Theory and Techniques Society. He has been named the Joseph M. Pettit Professor of Electronics in the School of Electrical and Computer Engineering at Georgia Tech. For the 2004–2006 term, he has been appointed an IEEE Distinguished Microwave Lecturer for his seminar entitled "Recent Advances in High Performance Communication Modules and Circuits."



Manos M. Tentzeris (S'89–M'98–SM'03) received the diploma degree in electrical and computer engineering (*magna cum laude*) from the National Technical University of Athens, Greece, and the M.S. and Ph.D. degrees in electrical engineering and computer science from the University of Michigan, Ann Arbor.

He was a Visiting Professor with the Technical University of Munich, Germany for the summer 2002, where he introduced a course in the area of high-frequency packaging. He is currently an Associate Professor with the School of Electrical and

Computer Engineering, Georgia Institute of Technology (Georgia Tech), Atlanta. He has helped develop academic programs in highly integrated/multilayer packaging for RF and wireless applications, microwave MEMs, SOP-integrated antennas and adaptive numerical electromagnetics (FDTD, multiresolution algorithms) and heads the ATHENA research group (15 researchers). He is the Georgia Tech NSF-Packaging Research Center Associate Director for RF Research and the RF Alliance Leader. He is also the leader of the RFID Research Group of the Georgia Electronic Design Center (GEDC) of the State of Georgia. He has given more than 40 invited talks in the same area to various universities and companies in Europe, Asia and America. He has published more than 180 papers in refereed journals and conference proceedings, eight book chapters, and he is in the process of writing three books.

Dr. Tentzeris is a member of the International Scientific Radio Union (URSI)-Commission D, an Associate Member of EuMA, and a member of the Technical Chamber of Greece. He was the recipient of the 1997 Best Paper Award of the International Hybrid Microelectronics and Packaging Society for the development of design rules for low-crosstalk finite-ground embedded transmission lines. He received the 2000 NSF CAREER Award for his work on the development of MRTD technique that allows for the system-level simulation of RF integrated modules, the 2001 ACES Conference Best Paper Award, the 2002 International Conference on Microwave and Millimeter-Wave Technology Best Paper Award (Beijing, China) for his work on Compact/SOP-integrated RF components for low-cost high-performance wireless front-ends, the 2002 Georgia Tech-ECE Outstanding Junior Faculty Award, the 2003 NASA Godfrey "Art" Anzic Collaborative Distinguished Publication Award for his activities in the area of finite-ground low-loss low-crosstalk coplanar waveguides, the 2003 IBC International Educator of the Year Award, the 2003 IEEE CPMT Outstanding Young Engineer Award for his work on 3D multilayer integrated RF modules, and the 2004 IEEE Transactions on Advanced Packaging Commendable Paper Award. He was also the 1999 Technical Program Co-Chair of the 54th ARFTG Conference, Atlanta, GA and he is the Vice-Chair of the RF Technical Committee (TC16) of the IEEE CPMT Society. He has organized various sessions and workshops on RF/Wireless Packaging and Integration in IEEE ECTC, IMS and APS Symposia in all of which he is a member of the Technical Program Committee in the area of "Components and RF." He is an Associate Editor of the IEEE TRANSACTIONS ON ADVANCED PACKAGING.